European Journal of Medicinal Chemistry 67 (2013) 60–63

Contents lists available at SciVerse ScienceDirect

European Journal of Medicinal Chemistry

journal homepage: http://www.elsevier.com/locate/ejmech

Short communication

Design, synthesis and cellular dynamics studies in membranes of a new coumarin-based "turn-off" fluorescent probe selective for Fe^{2+}

Olimpo García-Beltrán [a,b,*], Natalia Mena [c], Osvaldo Yañez [d], Julio Caballero [d], Víctor Vargas [a], Marco T. Nuñez [c], Bruce K. Cassels [a]

[a] Department of Chemistry, Faculty of Sciences, University of Chile, Santiago, Chile
[b] Departamento de Ciencias Químicas, Facultad de ciencias Exactas, Universidad Andrés Bello, Avenida República 275, Piso 3, Santiago, Chile
[c] Department of Biology, Faculty of Sciences, University of Chile, Santiago, Chile
[d] Centro de Bioinformática y Simulación Molecular, Facultad de Ingeniería, Universidad de Talca, 2 Norte 685, Casilla 721, Talca, Chile

ARTICLE INFO

Article history:
Received 16 April 2013
Received in revised form
25 May 2013
Accepted 4 June 2013
Available online 19 June 2013

Keywords:
Fe^{2+} ion
Turn-off probes
Fluorescent sensor
Molecular dynamics

ABSTRACT

A new coumarin-based 'turn-off' fluorescent probe, 7-(diethylamino)-*N*-(1,3-dihydroxy-2-(hydroxymethyl)propan-2-yl)-2-oxo-2*H*-chromene-3-carboxamide (**AGD**) was synthesized. This compound is highly selective for ferrous ions (Fe^{2+}) and can reversibly detect them in aqueous medium. The probe localizes to the cell membrane in living cells, where it can detect changes in Fe^{2+} concentration. Molecular dynamics (MD) simulations indicate that **AGD** interacts with the lipid bilayer at the level of the glycerol moieties.

Iron is widely distributed in nature and is one of the most important elements in biological systems, where it plays a crucial role in many biochemical processes at the cellular level. It is an essential element for the formation of the hemoglobin of vertebrate red cells and plays an important role in the storage and transport of oxygen to tissues [1]. It is also essential for many organisms and both its deficiency and excessive accumulation can induce various disorders such as anemia and damage to the liver and kidneys (due to hemochromatosis), which can eventually lead to liver cancer, cirrhosis, arthritis, diabetes and cardiac failure [2]. Recent studies show that elevated iron levels are associated with neurodegeneration such as that underlying Parkinson's disease [3], as well as in Friedreich's ataxia [4], and play a key role in some infectious diseases such as malaria [5] by participating through the various cytochromes in the electron transport chain and in the catabolism of endogenous and exogenous substances [1]. Iron is also detrimental as it fosters the generation of highly destructive oxygen species. Iron-dependent oxidative processes in cells are usually believed to be the result of increases in the release of superoxide anion radical ($O_2^{\cdot-}$) and/or H_2O_2 [6]. For all these reasons it is very important to be able to detect iron ions, particularly in cells. Several techniques such as atomic absorption spectroscopy, spectrophotometry and voltammetry have been used for iron assay. Some of them are complicated, and not suitable for quick and online monitoring [6,7]. In recent years, the development of sensitive chemosensors has become an active field of research because of their potential application in clinical biochemistry as well as analytical chemistry and environmental science [8]. Selective fluorescence chemosensors are especially important for monitoring biologically essential or toxic metal ions, such as Ca^{2+}, Zn^{2+}, Cu^{2+}, Mg^{2+}, Hg^{2+} and Pb^{2+} in cells [9]. Also, fluorescence sensors have attracted more and more attention due to their advantages over other techniques, including ease of detection, sensitivity, and instantaneous response.

In this work we report a new bifunctional probe derived from the fluorophore 7-diethylaminocoumarin and 2-amino-2-(hydroxymethyl)propane-1,3-diol as the ferrous iron-binding moiety. This probe, 7-(diethylamino)-*N*-(1,3-dihydroxy-2-(hydroxymethyl) propan-2-yl)-2-oxo-2*H*-chromene-3-carboxamide (**AGD**), is characterized by being water-soluble, binding to the cell membrane, and being reversible in the presence of more potent iron chelators.

* Corresponding author. Department of Chemistry, Faculty of Sciences, University of Chile, Santiago, Chile. Tel.: +56 2 29787253; fax: +56 2 22713888.
E-mail addresses: ojgarciab@ug.uchile.cl, ojgarciab@yahoo.com (O. García-Beltrán).

0223-5234/$ – see front matter © 2013 Elsevier Masson SAS. All rights reserved.
http://dx.doi.org/10.1016/j.ejmech.2013.06.022

The novel fluorescence probe was prepared *via* a conventional two-step synthesis from commercial precursors. 4-Diethylamino salicylaldehyde (**1**) was condensed with ethyl malonate (Knoevenagel) giving ethyl 7-diethylamino-2-oxo-2*H*-chromene-3-carboxylate (**2**). This coumarin was condensed with 2-amino-2-(hydroxymethyl)propane-1,3-diol (TRIS) to afford **AGD**, by analogy with a literature procedure (Scheme 1). The ^{1}H NMR and ^{13}C NMR spectra of **AGD** are available in the Supporting Information (Fig. 1A and B).

The absorption and emission spectral studies were performed in pH 7.4 HEPES buffer at room temperature. **AGD** shows an absorption maximum at 430 nm (Fig. 3; Supporting Information), a molar extinction coefficient (ε) of 5245 M^{-1} cm^{-1} and an emission band at 480 nm (Fig. 4; Supporting Information). The quantum yield of this probe is 0.103 and its Stokes shift is 2423 cm^{-1} Fe^{2+}, Fe^{3+}, Ca^{2+}, Co^{2+}, Mg^{2+}, Mn^{2+}, Zn^{2+}, Cd^{2+}, Pb^{2+} and Hg^{2+} chlorides were added at a final concentration of 200 μM to a 20 μM solution of **AGD**. The effects of all but Fe^{2+} and Fe^{3+} were negligible, and the fluorescence quenching by Fe^{2+} was about twice as intense as that of Fe^{3+} (Fig. 1). With excitation at 430 nm, the fluorescence emission intensity of **AGD** at 480 nm decreases by about one third upon increasing the concentration of Fe^{2+} from 0 to 200 μM (Fig. 2) and the quantum yield decreases to 0.0057. A good linear relationship between fluorescence intensity and Fe^{2+} concentration was observed, with a correlation coefficient as high as 0.99097 (Inset to Fig. 2).

The stability constant K_a of the **AGD**-Fe^{2+} interactions was determined using the Benesi–Hildebrand equation, which gives a value of 4.19×10^4 M^{-1} (Fig. 5; Supporting data). A literature report suggests that **AGD**-Fe^{2+} complexes might be polymeric, considering the steric effects, where an iron atom coordinates with the three hydroxyls of one **AGD** molecule and the two carbonyls of the following molecule (Fig. 6; Supporting data) [7]. The ESI spectrum exhibited a peak at *m/z* 420.3426 assignable to [**AGD** + Fe(II)]$^+$ (Fig. 7; Supporting data), indicative of a 1:1 stoichiometry, but it does not rule out the possibility of labile polymeric complexes. However, although the hydroxyl groups of the 2-amino-2-(hydroxymethyl) propane-1,3-diol, the carbonyl groups of the α-pyrone and amide, might all bind the iron atom in the monomeric species detected, the conformation adopted to form such a complex is unclear and should give rise to further work in coordination chemistry.

To assess the practical applicability of **AGD** as a Fe^{2+} selective fluorescent sensor, we carried out competitive experiments with 20 μM **AGD** pretreated with 200 μM of each of the following ions: Fe^{3+}, Zn^{2+}, Cu^{2+}, Co^{2+}, Ca^{2+}, Mn^{2+}, Mg^{2+}, Pb^{2+}, Cd^{2+}, and Hg^{2+}, after which 200 μM Fe^{2+} was added. As shown in Fig. 3, these experiments demonstrate that none of the selected ions interfere to any obvious extent with the detection of Fe^{2+}.

Fluorescent probes available for iron are few, and many of them cannot be used for biological applications. Moreover, bifunctional iron-chelating compounds with preference for a specific organelle are scarce, since the vast majority are found in the cytoplasm. Consequently, the behavior of **AGD** was studied in SH-SY5Y human neuroblastoma cells loaded with Fe^{3+} by incubating them for 24 h with ferric nitrilotriacetic acid complex (FeNTA), monitoring changes in fluorescence with a microplate fluorescence reader. Reversibility is another important feature of excellent chemical

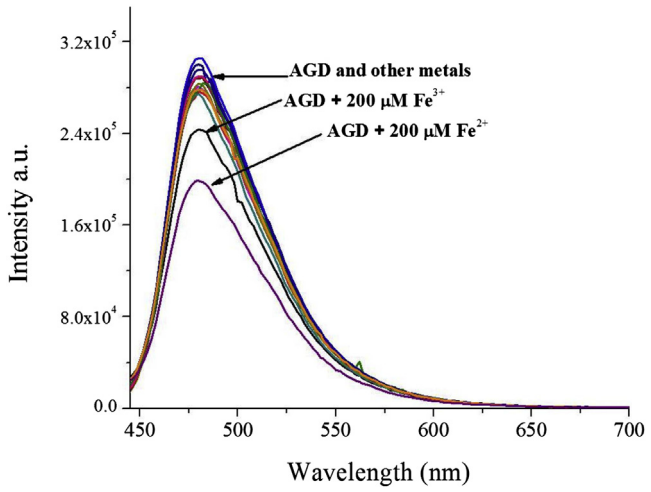

Fig. 1. Fluorescence spectra of **AGD** (20 μM) in the presence of different metal cations (200 μM) in 20 mM HEPES buffer, pH 7.4.

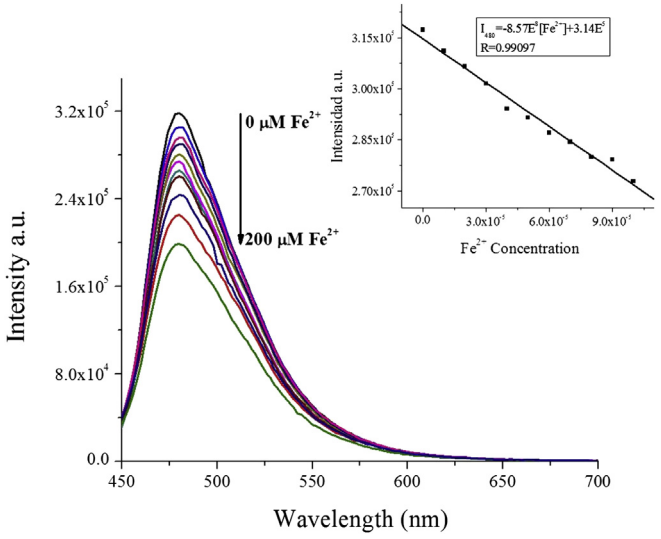

Fig. 2. Fluorescence spectra of **AGD** (20 μM) with different concentrations of Fe^{2+} in pH 7.4 HEPES buffer. Inset shows the relationship between fluorescence intensity and Fe^{2+} concentration (10–100 μM).

probes. Therefore, experiments were conducted adding bipyridyl (a molecule with high affinity for the metal) to examine the reversibility of the **AGD**-Fe^{2+} interaction (Fig. 4A). These showed that the fluorescence intensity of Fe–loaded cells treated with **AGD** (Fig. 4B) increased with the addition of bypiridyl (BIP, Fig. 4C). Subsequent addition of ferrous ammonium sulfate (FAS) quenched the fluorescence again (Fig. 4D). This experiment was also followed by epifluorescence microscopy, visualizing the change in fluorescence intensity caused by the different treatments. The mitochondria were labeled by incubation with Mito-Tracker (Fig. 5A). The

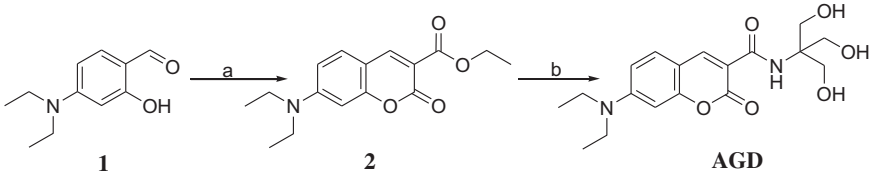

Scheme 1. Synthetic route to **AGD**. Reagents and conditions: a) diethyl malonate, piperidine, acetic acid, EtOH, reflux 6 h; b) 2-amino-2-hydroxymethylpropane-1,3-diol, EtOH, reflux 48 h.

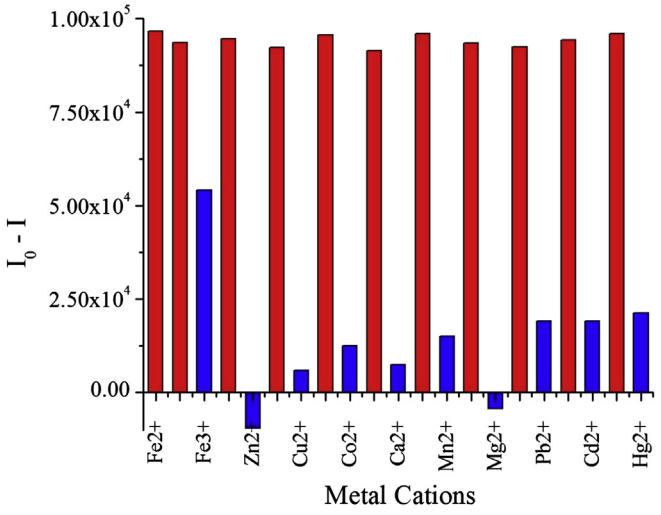

Fig. 3. Selectivity of the fluorescence quenching of **AGD** by Fe^{2+} in HEPES buffer pH 7.4. Blue bars indicate the fluorometric responses of **AGD** with 10 equiv of Fe^{3+}, Zn^{2+}, Cu^{2+}, Co^{2+}, Ca^{2+}, Mn^{2+}, Mg^{2+}, Pb^{2+}, Cd^{2+}, and Hg^{2+}. Red bars represent the florescence response after addition to the same solutions of 10 equiv. of Fe^{2+}. (For interpretation of the references to color in this figure legend, the reader is referred to the web version of this article.)

fluorescence due to **AGD** was concentrated in the cell membrane (Fig. 5B) with very little localization to the mitochondria, and a colocalization experiment (Fig. 5C) corroborated this observation.

A molecular dynamics (MD) simulation was performed in order to study the incorporation of **AGD** in the lipid phase of the cell membrane [10]. The conditions of the simulations and the software used are described in the Supplementary material. **AGD** was initially placed in the bulk water, far from the 1-palmitoyl-2-oleoyl-sn-glycero-3-phosphocholine (POPC) membrane. After 15 ns of simulation, **AGD** was incorporated into the lipid membrane (Fig. 6A). This process corresponds to the passive diffusion of the probe toward the membrane surface. After its incorporation, the more polar region of **AGD** (the {[2-hydroxy-1,1-bis(hydroxymethyl)ethyl]amino} carbonyl group and the oxygen atoms of the 2*H*-chromen-2-one scaffold) was positioned near the glycerol level of the lipid bilayer (Fig. 6). Analysis of the positions occupied by **AGD** during the MD simulation shows that this molecule does not enter into the depths of the membrane, and interacts only with the groups near the surface (Fig. 6B and zoom). We also evaluated the effect of **AGD** on the orientation of the membrane lipids. To do this we calculated the order parameter S_{CD} of the acyl chains of sn-1 and sn-2 POPC. Comparing pure POPC with the phospholipid containing **AGD**, we found that the sn-1 and sn-2 chains in the system containing **AGD** showed increased order (Figure S8; Supplementary data).

In conclusion, we have prepared and characterized a novel bifunctional fluorescence "turn-off" sensor that is highly sensitive and selective for reversible Fe^{2+} ion detection. This probe was used successfully to image cell membranes, responding to changes in available Fe^{2+} ion concentrations.

Acknowledgments

This work was supported by a postdoctoral fellowship from the Millennium Scientific Initiative (Grant P05-001-F). The authors thank the Instituto de Química de Recursos Naturales, Universidad de Talca, for the use of a mass spectrometer.

Appendix A. Supplementary data

Supplementary data related to this article can be found at http://dx.doi.org/10.1016/j.ejmech.2013.06.022.

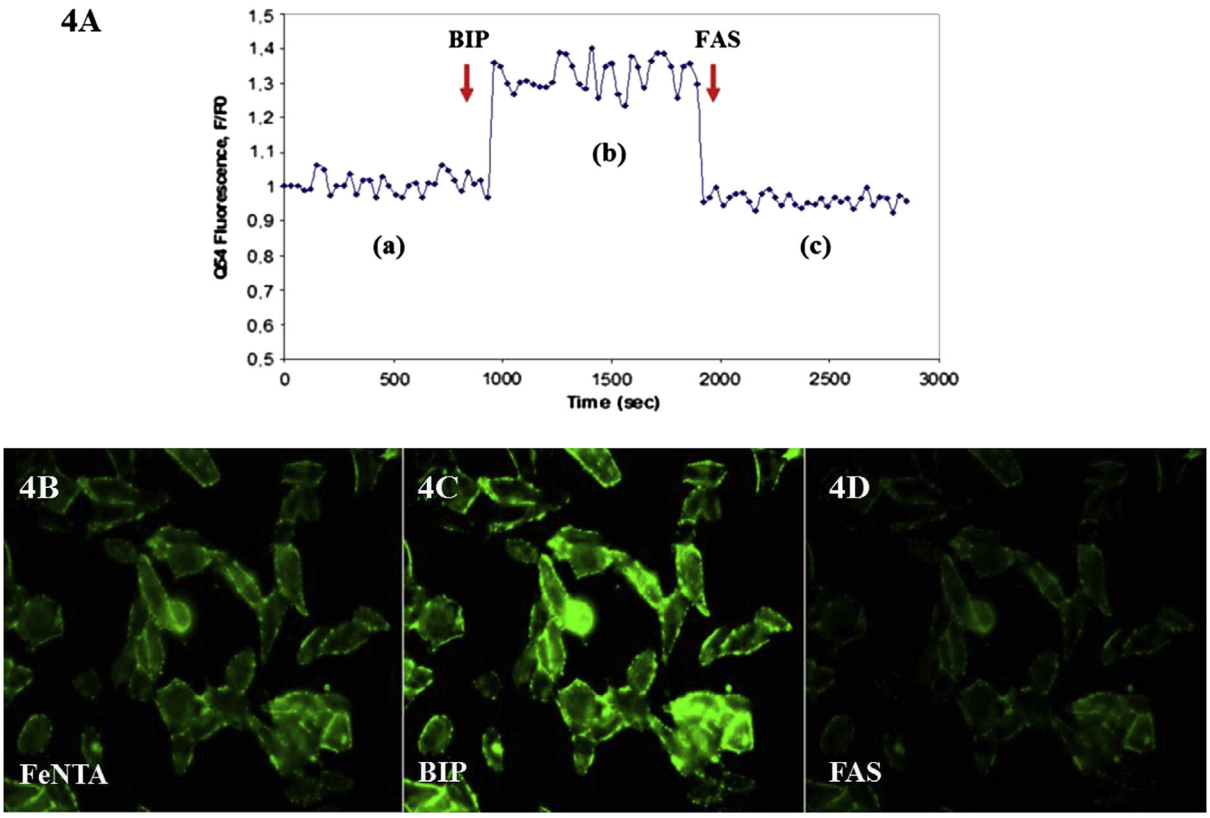

Fig. 4. (A) Fluorescence changes of **AGD** in SH-SY5Y cells. (B) Shows the basal fluorescence of the probe: SH-SY5Y cells were treated for 24 h with FeNTA (20 μM), and then incubated for 20 min with **AGD** (10 μM). (C) Fluorescence after adding BIP (20 μM), (D) Fluorescence after adding FAS (20 μM). Epi-fluorescence microscope, 63×.

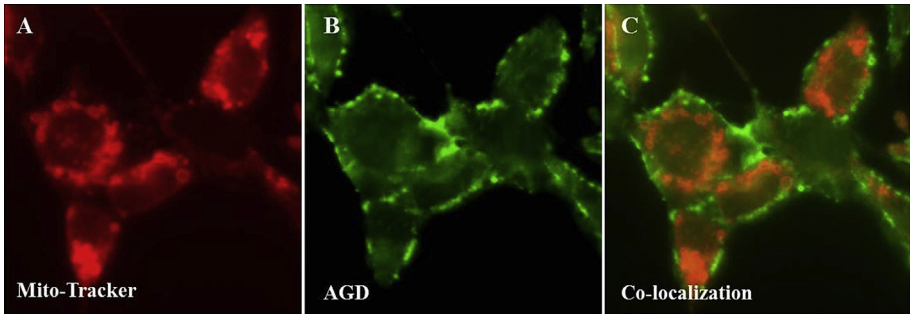

Fig. 5. (A) SH-SY5Y cells treated with Mito-tracker. (B) SH-SY5Y cells treated with **AGD** (5 μM). (C) Different localization of both probes. 63× objective.

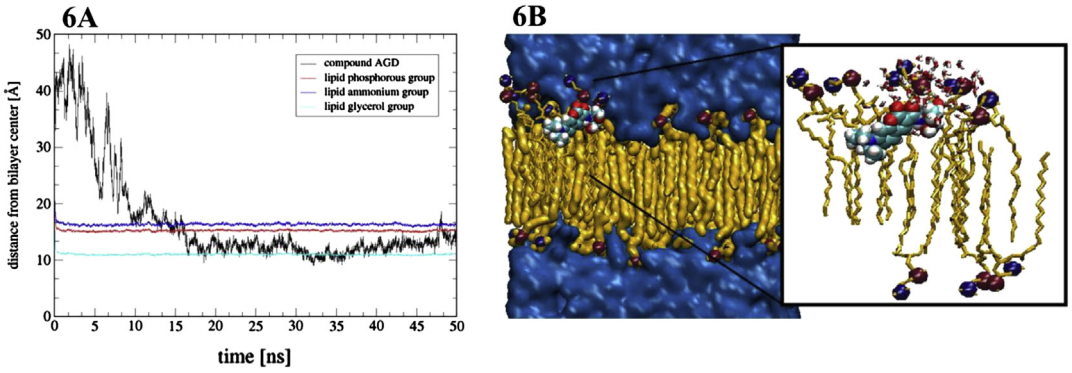

Fig. 6. The dependence of the AGD center of mass position as a function of time of unconstrained MD simulation. (A) Location of AGD is depicted by a black curve. The positions of the ammonium (blue curves), phosphate (red curves) and glycerol (cyan curves) moieties of the lipid bilayer are also plotted. (B) Typical snapshot of a POPC bilayer containing **AGD** from MD simulations. A zoomed snapshot is also shown. (For interpretation of the references to color in this figure legend, the reader is referred to the web version of this article.)

References

[1] X.B. Zhang, G. Cheng, W.J. Zhang, G.L. Shen, R.Q. Yu, A fluorescent chemical sensor for Fe^{3+} based on blocking of intramolecular proton transfer of a quinazolinone derivative, Talanta 71 (2007) 171–177.
[2] C. Brugnara, Iron deficiency and erythropoiesis: new diagnostic approaches, Clin. Chem. 49 (2003) 1573–1578.
[3] J. Beard, Iron deficiency alters brain development and functioning, J. Nutr. 133 (2003) 1468S–1472S.
[4] L. Zecca, M.B. Youdim, P. Riederer, J.R. Connor, R.R. Crichton, Iron, brain ageing and neurodegenerative disorders, Nat. Rev. Neurosci. 5 (2004) 863–873.
[5] T.J. Egan, R. Hunter, C.H. Kaschula, H.M. Marques, A. Misplon, J. Walden, Structure–function relationships in aminoquinolines: effect of amino and chloro groups on quinoline–hematin complex formation, inhibition of β-hematin formation, and antiplasmodial activity, J. Med. Chem. 43 (2000) 283–291.
[6] F. Petrat, D. Weisheit, M. Lensen, H. de Groot, R. Sustmann, U. Rauen, Selective determination of mitochondrial chelatable iron in viable cells with a new fluorescent sensor, Biochem. J. 362 (2002) 137–147.
[7] J. Yao, W. Dou, W. Qin, W. Liu, A new coumarin-based chemosensor for Fe^{3+} in water, Inorg. Chem. Commun. 12 (2009) 116–118. (For some examples, see:);
(a) B. Espósito, S. Epsztejn, W. Breuer, Z.I. Cabantchik, A review of fluorescence methods for assessing labile iron in cells and biological fluids, Anal. Biochem. 304 (2002) 1–18;
(b) F. Petrat, U. Rauen, H. de Groot, Determination of the chelatable iron pool of isolated rat hepatocytes by digital fluorescence microscopy using the fluorescent probe, phen green SK, Hepatology 29 (1999) 1171–1179;
(c) W. Luo, Y.M. Ma, P.J. Quinn, R.C. Hider, Z.D. Liu, Design, synthesis and properties of novel iron(III)-specific fluorescent probes, J. Pharm. Pharmacol. 56 (2004) 529–536;
(d) Y. Ma, W. Luo, P.J. Quinn, Z. Liu, R.C. Hider, Design, synthesis, physicochemical properties, and evaluation of novel iron chelators with fluorescent sensor, J. Med. Chem. 47 (2004) 6349–6362;
(e) Y. Ma, Z. Liu, R.C. Hider, F. Petrat, Determination of the labile iron pool of human lymphocytes using the fluorescent probe, CP655, Anal. Chem. Insights 2 (2007) 61–67;
(f) S. Fakih, M. Podinovskaia, X. Kong, H.L. Collins, U.E. Schaible, R.C. Hider, Targeting the lysosome: fluorescent iron(III) chelators to selectively monitor endosomal/lysosomal labile iron pools, J. Med. Chem. 51 (2008) 4539–4552;
(g) Y. Ma, W. Luo, M. Camplo, Z. Liu, R.C. Hider, Novel iron-specific fluorescent probes, Bioorg. Med. Chem. Lett. 15 (2005) 3450–3452.
[8] H.-Y. Li, Sh. Gao, Zh. Xi, A colorimetric and "turn on" fluorescent chemosensor for Zn(II) based on coumarin Schiff-base derivatives, Inorg. Chem. Commun. 12 (2009) 300–303.
[9] Sh. Bae, J. Tae, Rhodamine-hydroxamate-based fluorescent chemosensor for Fe^{III}, Tetrahedron Lett. 48 (2007) 5389–5392.
[10] J. Barucha-Kraszewska, S. Kraszewski, P. Jurkiewicz, Ch. Ramseyer, M. Hof, Numerical studies of the membrane fluorescent dyes dynamics in ground and excited states, Biochim. Biophys. Acta 1798 (2010) 1724–1734.